American Journal of Infection Control 44 (2016) S127-S137

Contents lists available at ScienceDirect

American Journal of Infection Control

journal homepage: www.ajicjournal.org

Major Article

Mathematical modeling and simulation of bacterial distribution in an aerobiology chamber using computational fluid dynamics

Bahram Zargar BSc(Engg), MSc(Engg), PhD [a], Farshad M. Kashkooli BSc(Engg), MSc(Engg) [b], M. Soltani BSc(Engg), MSc(Engg), PhD [b,c], Kathryn E. Wright MA, MSc, PhD [a], M. Khalid Ijaz DVM, MSc(Honors), PhD [d,e], Syed A. Sattar MSc, Dip Bact, MS, PhD [f,*]

[a] Department of Biochemistry, Microbiology, and Immunology, University of Ottawa, Ottawa, Ontario, Canada
[b] Department of Mechanical Engineering, K. N. T. University of Technology, Tehran, Iran
[c] Division of Nuclear Medicine, Department of Radiology and Radiological Science, Johns Hopkins University, School of Medicine, Baltimore, MD
[d] RB, Montvale, NJ
[e] Department of Biology, Medgar Evers College of the City University of New York (CUNY), Brooklyn, NY
[f] Professor Emeritus of Microbiology, Faculty of Medicine, University of Ottawa, Ottawa, ON, Canada

Key Words:
Airborne spread of infectious agents
Distribution of particles in indoor air
Sampling air for infectious agents
Predictive modeling of bacterial distribution in an aerobiology chamber

Background: Computer-aided design and draft, along with computer-aided engineering software, are used widely in different fields to create, modify, analyze, and optimize designs.
Methods: We used computer-aided design and draft software to create a 3-dimensional model of an aerobiology chamber built in accordance with the specifications of the 2012 guideline from the Environmental Protection Agency for studies on survival and inactivation of microbial pathogens in indoor air. The model was used to optimize the chamber's airflow design and the distribution of aerosolized bacteria inside it.
Results: The findings led to the identification of an appropriate fan and its location inside the chamber for uniform distribution of microbes introduced into the air, suitability of air sample collection from the center of the chamber alone as representative of its bacterial content, and determination of the influence of room furnishings on airflow patterns inside the chamber.
Conclusions: The incorporation of this modeling study's findings could further improve the design of the chamber and the predictive value of the experimental data using it. Further, it could make data generation faster and more economical by eliminating the need for collecting air samples from multiple sites in the chamber.

INTRODUCTION

Prediction of particle transport in turbulent flow is essential in different fields, such as dispersion of passive or reactive particles in turbulent media and in studying air pollution.[1] For example, we are exposed to airborne particulates in workplaces, homes, and other indoor settings.[2] The fate and deposition of such particulates indoors have substantial implications for human and animal health, clean rooms, and air decontamination.[3-5] Therefore, a good understanding of the particle-laden turbulent flow is important in addressing indoor air quality issues and in controlling particle dispersion.

Mitigating the spread of microbial contaminants by indoor air is an essential design consideration for homes, biomedical and health care facilities, and other public settings. Once airborne, the movement of microbes is difficult to control because they may become rapidly dispersed by air movement or adhere to other surfaces for travel with them.[6,7] Ventilation, either natural or mechanical, can provide adequate air exchanges to reduce the risk for airborne microbial spread; however, mechanical ventilation, particularly with conditioning, can be expensive.[8] According to the *Guidelines for Design and Construction of Hospital and Health Care Facilities*,[9] 6-15 air changes per hour are needed to maintain a healthful environment while reducing exposure to harmful chemicals and microbes. This

* Address correspondence to Syed A. Sattar, MSc, Dip Bact, MS, PhD, Professor Emeritus of Microbiology, Faculty of Medicine, University of Ottawa, 451 Smyth Rd, Ottawa, ON K1H 8M5, Canada.
E-mail address: ssattar@uottawa.ca (S.A. Sattar).
Funding/Support: This paper was presented at a workshop organized under the auspices of ASTM International's biannual meeting held in April 2016. Publication of this supplement is primarily supported by RB, Montvale, New Jersey, with additional support from MicroBioTest, a division of Microbac Laboratories, Inc., Sterling, Virginia. The City University of New York (CUNY) and the University of Ottawa, Ottawa, Canada, are academic sponsors. Editorial support was provided by Ashley O'Dunne, PhD; Shannon O'Sullivan, ELS; and Alanna Franchetti, ELS of Medergy (Yardley, PA), and funded by RB.

0196-6553/
http://dx.doi.org/10.1016/j.ajic.2016.06.005

requires ventilation system engineers to understand microbial behavior in air to design more efficient and economical means of treating and supplying indoor air.[10]

In general, particles with a mass median aerodynamic diameter of 10 μm or less can remain airborne.[11] Memarzadeh and Xu[12] emphasized the importance of particle size in the airborne transmission of infections by transport of pathogen-laden particles to the mucosal surface of a susceptible host.[12]

Available information shows that ventilation systems can influence the spread of airborne pathogens indoors,[13,14] airflow patterns may contribute directly to such spread,[15] and airflow rates can influence the transport and removal of human expiratory droplets.[5,16-18] Assessing the risk of transmission of infections via air is more difficult than predicting reductions in concentrations of harmful gases with ventilation. Also, and unlike inhaled gases, it may take only a few infectious units of a given pathogen to infect a susceptible host, which, in turn, can amplify the level of the pathogen many-fold for further dissemination.

Increasing the air exchange rate alone is often inadequate for reducing the risk of spread of airborne infections everywhere within a given room. For optimal safety, the entire ventilation system should be analyzed to determine the likely path of pathogen-laden particulates within the occupied zones and the required corrective action.[19]

The 2 major approaches to study of the dispersion of particles in indoor air are physical modeling and numerical simulation with computational fluid dynamics (CFD). Empirical data are useful for CFD validation of air and movement of particulates in indoor environments and health care facilities. CFD modeling is also much more economical to perform than full-scale experimentation with actual pathogens or their surrogates.[20] Thus, with the ready availability and greater sophistication of CFD, it is increasingly being applied to predict room air movement in various types of health care settings.[21] However, this approach has not been adequately applied to other types of indoor settings and validated with experimental data[22]; when applied to predict airflow patterns in buildings, it was a flexible alternative to physical models.[22-24]

This study applies CFD to optimize and validate the performance of an aerobiology chamber that was designed based on Environmental Protection Agency guidelines.[25] The best location, angle, and speed of a muffin fan for producing uniform bacterial distribution were determined. The number of air sampling sites required for characterizing the distribution of the nebulized bacteria in the chamber was investigated. The stabilization time required to produce a uniform distribution of the bacteria was determined, and the effect of furniture on bacterial distribution also was studied.

METHODS

The dimensions of the studied aerobiology chamber were 320 cm × 360 cm × 210 cm.[26] The chamber was designed based on Environmental Protection Agency guidelines[25] and then used to study bacteria survival in air (Fig 1).[26] A 6-jet nebulizer was used to aerosolize bacterial suspensions into the chamber through a pipe with a 3.8-cm diameter. The air was sampled from the center of the chamber using a slit-to-agar machine via a 5.0-cm pipe. A muffin fan (Nidec Alpha V, TA300, Model A31022-20, P/N: 933314 3.0-inch/7.62-cm diameter; output 30 CFM; Nidec Corp., Braintree, MA) placed on the floor of the chamber directly beneath the nebulizer inlet pipe was actuated from the outside for continuous operation during nebulization and testing to ensure uniform distribution of the aerosolized particles and/or any treatment introduced. The procedure of the experiment was as follows:

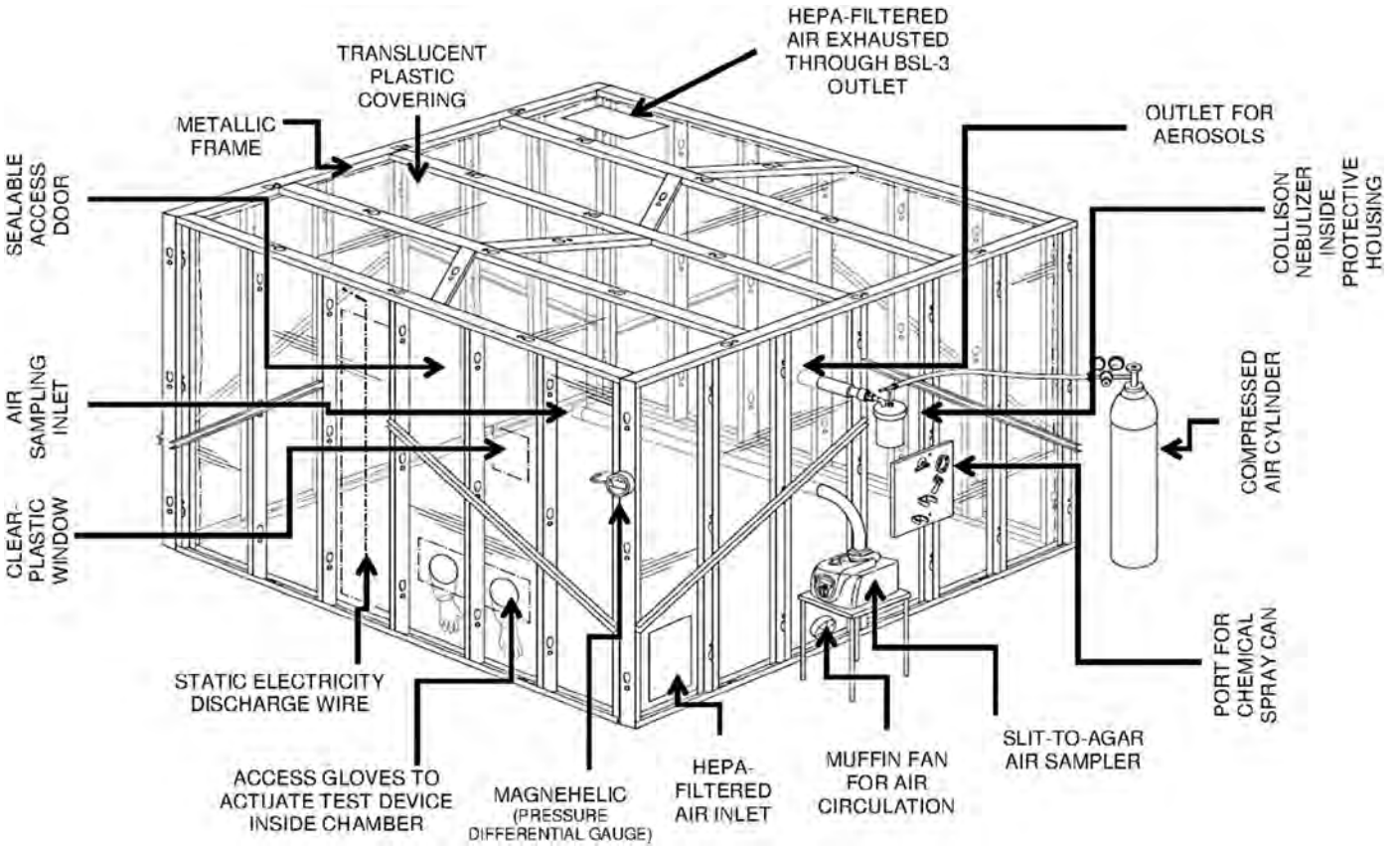

Fig 1. Aerobiology chamber designed based on Environmental Protection Agency guidelines.[25] Reprinted with permission.

- The fan was activated at least 300 seconds before the experiment to circulate the air inside the chamber;
- The test bacterial suspension was nebulized into the chamber for 10 minutes using a 6-jet collison nebulizer; and
- Before sampling, the air in the chamber was allowed to circulate for 300 seconds following the nebulization process.

MATHEMATICAL MODELING, MATERIALS, AND NUMERIC METHODOLOGIES

Theoretical background

The Eulerian-Lagrangian approach was implemented directly using the discrete phase model. In this approach, the fluid phase is treated as a continuum material by solving the time-averaged Navier-Stokes equations, and the dispersed phase is solved by tracking a large number of particles through the calculated flow field.[27] The governing equations are itemized in the following sections.

Governing equations for the continuous phase

The continuous gas-flow phase is governed by the following equations for unsteady compressible flow:[4]

- Continuity equation:

$$\frac{\partial \rho}{\partial t} + \nabla \cdot (\rho \vec{u}) = 0 \tag{1}$$

- Momentum equation:

$$\frac{D(\rho \vec{u})}{Dt} = -\vec{\nabla} p + \nabla \cdot \tau \tag{2}$$

- Energy equation:

$$\frac{\partial (\rho E)}{\partial x} + \nabla \cdot (\vec{u}(\rho E + p)) = \nabla \cdot (k_{eff} \nabla T + (\vec{\tau}_{eff} \cdot \vec{u})) \tag{3}$$

Where ρ, t, u, r, p, τ, E, T, k_{eff}, and τ_{eff} are fluid density, time, fluid phase velocity, thermodynamic pressure, stress tensor, energy, temperature, effective conductivity, and effective stress tensor, respectively.

One of the most common turbulence models, the k-ε Realizable turbulence model, was used for turbulence modeling. The turbulence kinetic energy, k, and its rate of dissipation, ε, are obtained from the following transport equations:[27,28]

$$\frac{\partial}{\partial t}(\rho k) + \frac{\partial}{\partial x_i}(\rho k u_j) = \frac{\partial}{\partial x_i}\left[\left(\mu + \frac{\mu_t}{\sigma_k}\right)\frac{\partial k}{\partial x_j}\right] + G_k + G_b - \rho\varepsilon - Y_M + S_k \tag{4}$$

$$\frac{\partial}{\partial t}(\rho \varepsilon) + \frac{\partial}{\partial x_j}(\rho \varepsilon u_j) = \frac{\partial}{\partial x_j}\left[\left(\mu + \frac{\mu_t}{\sigma_\varepsilon}\right)\frac{\partial \varepsilon}{\partial x_j}\right] + \rho C_1 S_\varepsilon - \rho C_2 \frac{\varepsilon^2}{k + \sqrt{\upsilon \varepsilon}} + C_{1\varepsilon}\frac{\varepsilon}{k} C_{3\varepsilon} G_b + S_\varepsilon \tag{5}$$

Where G_k and G_b represent the generation of k due to the mean velocity gradients and buoyancy, respectively; Y_M represents the contribution of the fluctuating dilation in compressible turbulence to the overall dissipation rate; σ_k and σ_ε are the turbulent Prandtl numbers for k and ε, respectively; and S_k and S_ε are user-defined source terms for k and ε, respectively.

The turbulent (or eddy) viscosity, μ_t, is computed by combining k and ε as follows:[27,28]

$$\mu_t = \rho C_\mu \frac{k^2}{\varepsilon} \tag{6}$$

The model constants $C_{1\varepsilon}$, $C_{2\varepsilon}$, C_μ, σ_k, and σ_ε have the following values: $C_{1\varepsilon} = 1.44$, $C_{2\varepsilon} = 1.92$, $C_\mu = 0.09$, $\sigma_k = 1.0$, and $\sigma_\varepsilon = 1.3$.[27,28]

The rotating reference frame was applied only in the rotational region by assuming that the region was in a quasisteady state. This method does not explicitly generate model rotation; instead, it generates a constant grid flux in the appropriate conservation equations by automatically adding the source terms with respect to the Coriolis force and centrifugal force, which are calculated with equation 7 based on the properties of the reference frame.[27] Although this method underestimates the weak effect, it is appropriate for the flow, which is most likely to be influenced by time-averaged properties.[27] A significant amount of simulation time can be saved with this method, when compared with simulating the axial flow fan's rotation in a transient state.[27]

$$F_r = \rho \omega \times v \tag{7}$$

Where F_r is the body force term due to fan rotation (kg/m^2/s^2), ρ is the air density (kg/m^3), ω is the rotational speed (rad/s), and v is the linear velocity (m/s).

Governing equations for the discrete phase

The trajectory of the discrete phase is determined by integrating the force balance on the particle, which equates the particle inertia with forces acting on the particle, and can be written as:[27]

$$\frac{du_p}{dt} = F_D(u - u_p) + \frac{g_x(\rho_p - \rho)}{\rho_p} + F_x \tag{8}$$

Where u, u_p, g_x, ρ_p, ρ, and F_x are the fluid phase velocity, particle velocity, gravitational acceleration, particle density, fluid density, and an additional acceleration (force per unit particle mass), respectively. The drag force per unit particle mass (F_D) is equal to:

$$F_D = \frac{18\mu}{\rho_P d_p^2}\frac{C_D Re}{24} \tag{9}$$

$$Re \equiv \frac{\rho d_p |u_p - u|}{\mu} \tag{10}$$

Where μ, d_p, C_D, and Re are the molecular viscosity of the fluid, particle diameter, drag coefficient, and Reynolds number, respectively. The location of each particle, x, is tracked with the following equation:

$$\frac{dx}{dt} = u_p \tag{11}$$

The air velocity, u, in equation 8 is composed of the time-averaged component, $\bar{u}$, and the instantaneous or fluctuating velocity component, $u'(t)$:[4,27]

$$u = \bar{u} + u'(t) \tag{12}$$

The u component is computed using the Reynolds-averaged Navier-Stokes equations with the k-ε Realizable turbulence model. The u′(t) component is computed using a stochastic approach, such as the discrete random walk model or eddy lifetime model.[4] Its value prevails during the lifetime of the turbulent eddy influencing the particle and is assumed to obey the Gaussian probability distribution.[4] Using the discrete random walk model to calculate u′(t), the particle turbulent dispersion is correlated to the flow k:[4,27]

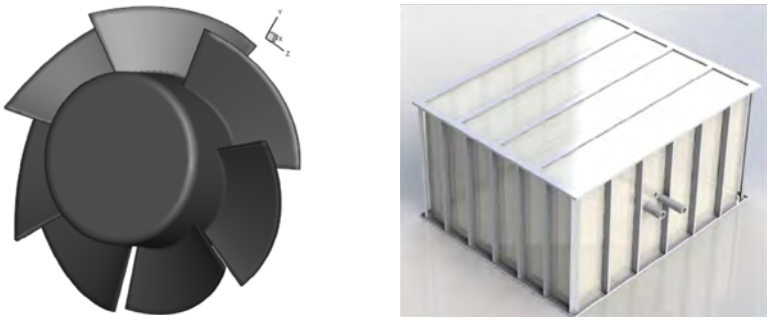

(a) Axial flow fan model (b) Computational domain (aerobiology chamber) model

Fig 2. Three-dimensional model of the axial flow fan and computational domain.

$$u'(t) = \zeta\sqrt{\frac{2k}{3}} \quad (13)$$

Where the variable ζ is a Gaussian random number.

CFD procedure

Generally, flow simulations in CFD take place in 3 main stages. The first step is preprocessing, which includes geometric modeling, production of computational domain, and grid generation. The second is the processing step or flow solution with CFD. In the final step, called postprocessing, the results are displayed.

Geometric modeling

The geometry of the aerobiology chamber consists of several components, such as axial flow fan, fan housing, air sampler inlet pipe, outlet pipe for aerosol sampling, and aerobiology chamber walls. Each of these geometries is modeled separately, and eventually, with superposition of the modeled geometries, the final complex geometry is generated. The computer-aided design and draft model of the flow region is built based on the computer-aided design and draft model of the aerobiology chamber.

The muffin fan, which is an axial flow fan, presents the most complex geometry in the system. The axial flow fan is a tube-axial device with 7 forward-swept blades. The dimension of the fan housing is 80 mm × 80 mm × 40 mm. The tip diameter of fan blades, hub-to-tip ratio, and tip clearance are 76 mm, 0.566 mm, and 1 mm, respectively. Figure 2a presents a 3-dimensional model of the fan.

The whole computational model is shown in Figure 2b. To achieve a reasonable numeric accuracy, it is divided into its different parts. The computational domain is composed of the axial flow fan, fan housing, air sampler inlet pipe, outlet pipe for aerosols, and aerobiology chamber, as shown in Figure 2b.

Grid generation

The physical model of the aerobiology chamber comprises several components with very different geometries. Because of the complicated geometry, unstructured tetrahedral grids were adopted for the whole computational domain. Grids of different sizes were generated for different components and then connected to form the whole geometry. The computational meshes of the aerobiology chamber were divided into 2 zones: rotating zone and stationary zone. Special attention was paid to the geometry and meshing of the fan, with the greatest emphasis on the blades and root of the blades. The rotating zone was a cylindric mesh with 531,218 cells, as shown in Figure 3. Meshes of the surfaces of the axial flow fan

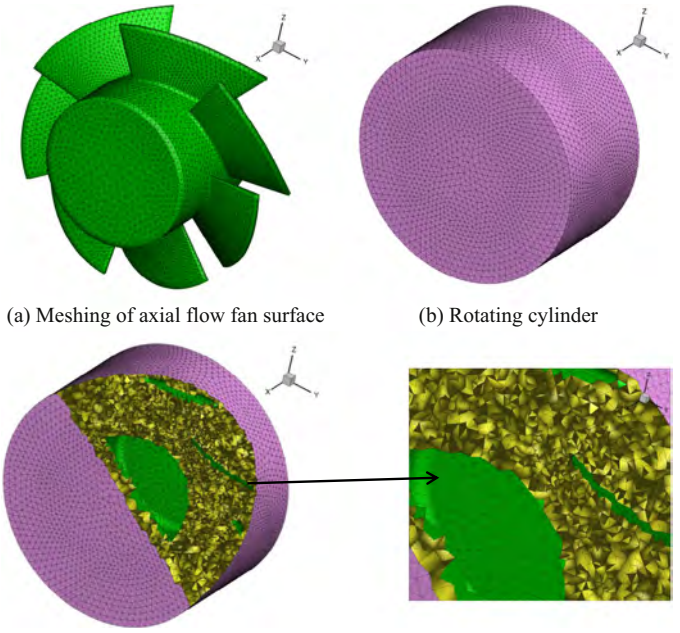

(a) Meshing of axial flow fan surface (b) Rotating cylinder

(c) Cut view of the volume meshing in rotating cylinder

Fig 3. Grid generation in rotating volume.

are also shown in Figure 3. The stationary zone contained 1,125,612 cells.

Several versions of the computational mesh were generated to test the grid independence. Results of this study of the grid are shown in Figure 4. The volume flow rates for cases 3-6 were almost the same. Because case 3 had the lowest computational costs, it was considered the optimum grid number. For a mesh with 1.04 million cells, the maximum cell skewness was 162, and with mesh size of 1.65 million cells, the maximum cell skewness decreased to 154. Thus, the mesh density had an effect on the results for the control simulation case.

Solver

Steady and unsteady simulations

Considering the rotating speed of the axial fan, the airflow was assumed incompressible.[27] The 3-dimensional incompressible Navier-Stokes equations and the k–ε Realizable model were used to model the effects of turbulence on the flow field. The enhanced wall function was used for boundary layer calculation. The second-order upwind differencing format for the convection terms of each

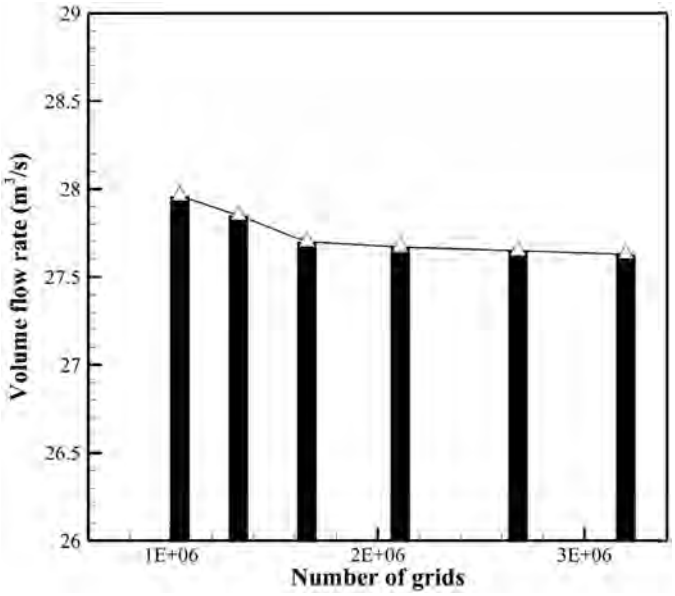

Fig 4. Mesh independency of aerobiology chamber with fan working at 2,500 rpm.

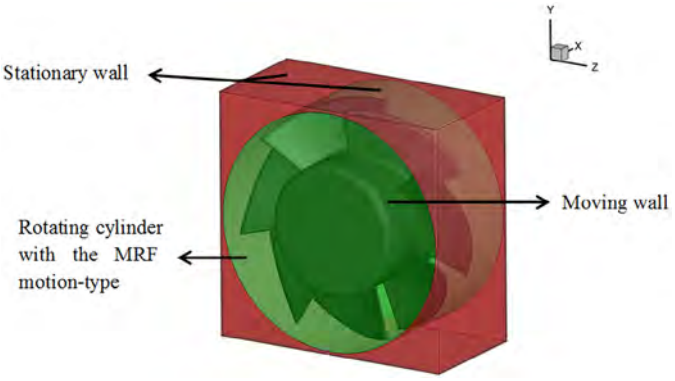

Fig 5. Boundary conditions of fan and its housing. *MRF*, multiple rotating reference frames.

governing equation was adopted, and the second-order accuracy was maintained for the viscous terms. The pressure-velocity coupling was handled by the SIMPLE algorithm for steady solutions and SIMPLEC for unsteady solutions. Because of the large number of computational cells and the possible presence of dynamic effects due to fan rotation, the convergence was satisfied with the criterion of 1×10^{-5} and, in some cases, with the criterion of 5×10^{-6}.

Boundary conditions

The inlet and outlet faces of the fan were set to the interior. No-slip condition was applied on the solid walls. In this simulation, it was assumed that the walls had zero velocity relative to the adjacent fluid. The flowing domain was divided into 2 parts: rotating body and flowing channel. A rotating reference frame was applied to the rotating region around the propeller fan. Different angular velocities were assigned to the rotary zone in the multiple rotating reference frames. A fixed reference frame was applied to the static regions. The conformal interfaces were used for rotor–stator interfaces to accelerate computation speed and improve accuracy. Figure 5 illustrates the boundary conditions of the fan and its housing. Also, the walls of the aerobiology chamber were regarded as stationary.

Turbulence models

Reynolds number was defined based on the fan radius and rotational speed as:[27]

$$\mathrm{Re} = \frac{R^2\omega}{\nu} \tag{14}$$

Where R, ω, and ν are fan radius, rotational speed, and kinematic viscosity, respectively. The Reynolds number of the airflow at a rotational speed of 2,500 rpm was 60,136, which represented a turbulent flow. That is, the existence of the fan as a rotating machine caused a turbulent flow in the chamber. In such a flow, the terms representing turbulence stress should be modeled and added to Navier-Stokes equations. A turbulence model of k–ε Realizable was used to analyze the flow disturbance in the aerobiology chamber. When the fan is operating, its induced momentum is crucial to the airflow and turbulence predictions. Therefore, a low Reynolds number variation of the k–ε Realizable model was used. Flow was solved in 3 rotational fan speeds to select the best velocity for producing uniform flow. The turbulence effects on the particles were accounted for using the discrete random walk model.[27] In addition, it was assumed in the simulations that the particles would rebound to the air after collision with any solid surface.

Postprocessing of the simulation results

The particle trajectories were tracked at different times after particle injection. The nature of the Eulerian-Lagrangian simulation provided for tracking every particle parcel in the flow field at any time.[4] Each parcel that contained a large number of particles was mathematically symbolized as a point in the Eulerian-Lagrangian simulation and represented as a dot in the postprocessed results.[4]

Five different planes passing through the center of the chamber were considered in calculating the area-weighted average velocity magnitude (Fig 6). In a state of uniform flow, the average velocity magnitude in different planes should not be significantly different.

To evaluate bacteria distribution inside the chamber, 5 different control volumes were considered. Each volume was a cube with the dimensions 1 m × 1 m × 1 m (Fig 7). The mass concentrations of particles and the number concentration of particles were calculated. In this study, the number of parcels within the control volume was counted manually. Then, based on the number of parcels, the particle concentrations (number and mass) were determined.

Simulation cases

Twelve configurations of fan position, angle, and velocity were considered (Table 1). The fluid flow was studied in each case with and without injection of aerosolized bacteria. The bacteria distribution and airflow were compared to find the case that could best produce uniformity. To study the effect of furniture on the airflow and bacteria distribution, basic bedroom furniture (ie, a bed, a chair, and a desk) was added to the chamber. The bacteria distribution was then compared with that in an empty room.

RESULTS AND DISCUSSION

Figure 8 compares the 3-dimensional pathlines of the aerobiology chamber for cases 3 and 12. Figures 8a, 8c, and 8d show a vortex, which is not desirable for uniform airflow, whereas Figure 8b is the only case showing no vortex. Such a comparison made between the 3-dimensional pathlines of all cases defined in Table 1 found state 1 (cases 1, 2, and 3) to be the only state with no vortices. This implied that there was uniform airflow when the fan was sitting at a 45° angle in the middle of 1 side of the chamber.

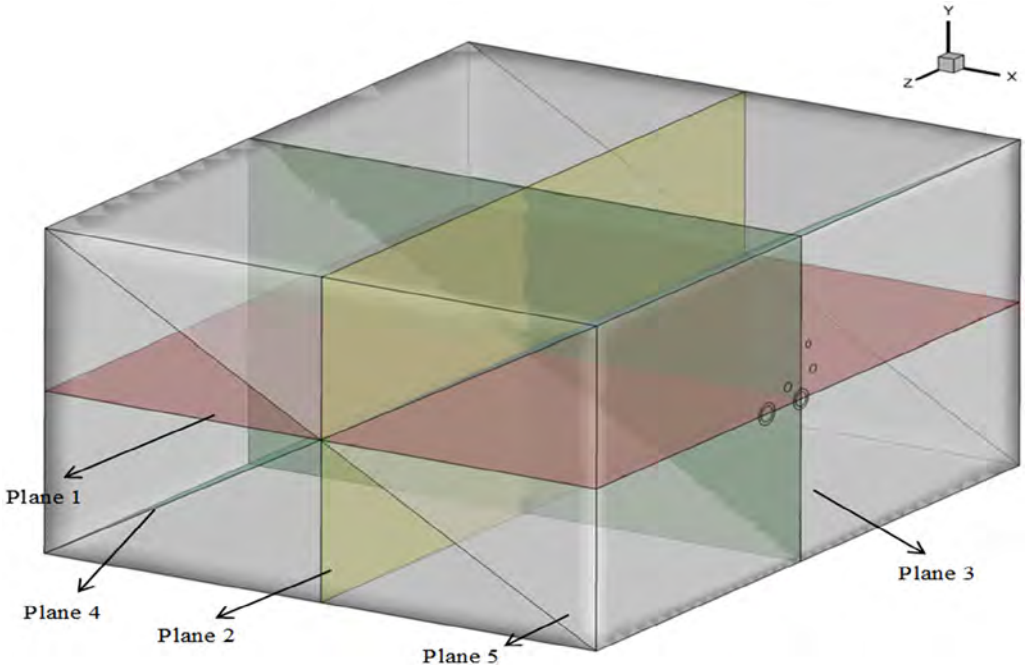

Fig 6. Locations of 5 different planes passing through the center of the aerobiology chamber.

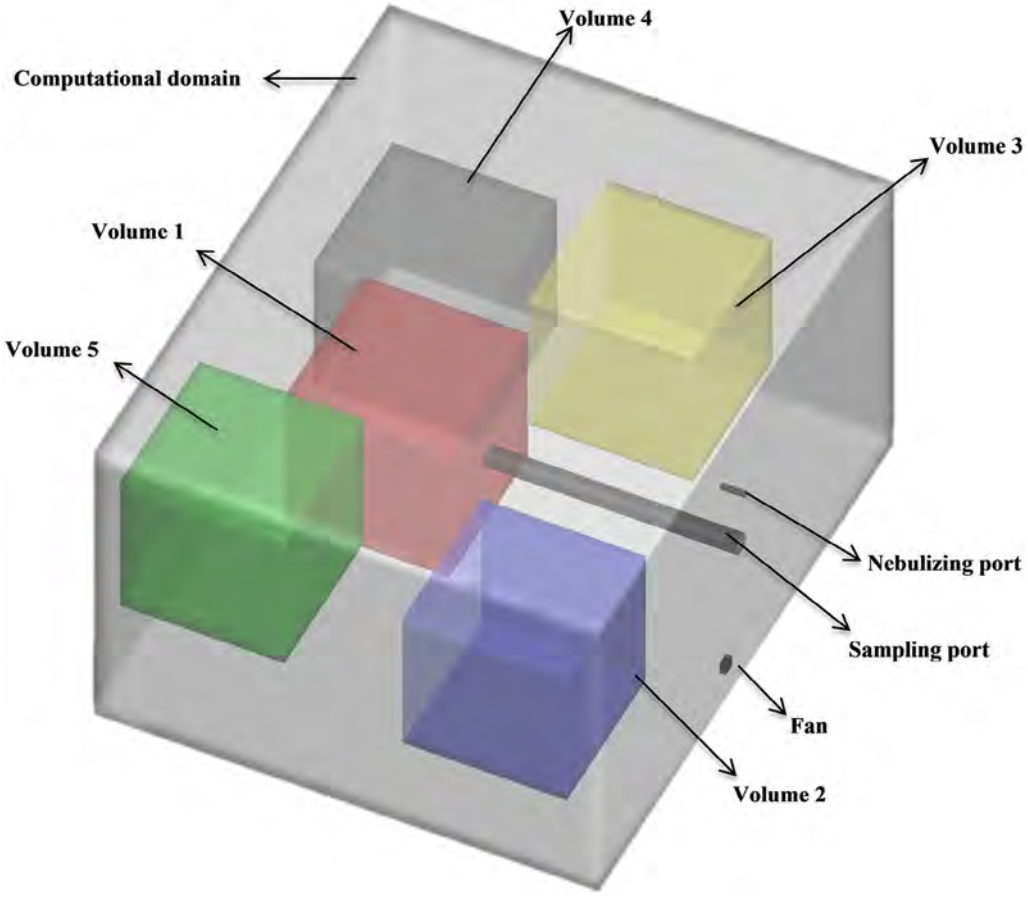

Fig 7. Computational domain and 5 volumes that were considered as samples.

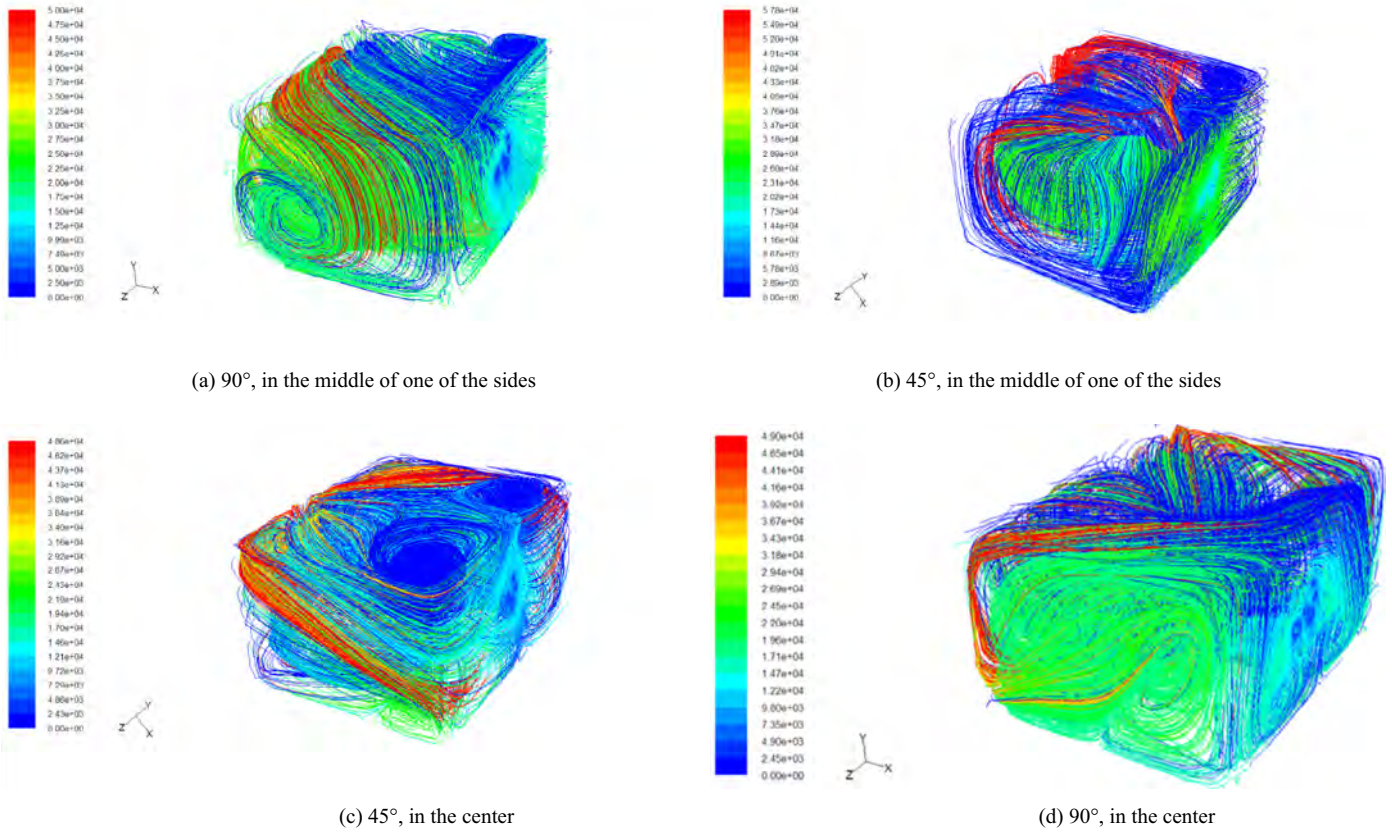

(a) 90°, in the middle of one of the sides

(b) 45°, in the middle of one of the sides

(c) 45°, in the center

(d) 90°, in the center

Fig 8. The pathlines of the aerobiology chamber for the velocity of 2,800 rpm.

Table 1
Different combinations (cases) of position, angle, and speed of the muffin fan

State	Case	Rotational speed (rpm)	Angle	Position
1	1	2,300	45°	In the middle of 1 of the sides
	2	2,500		
	3	2,800		
2	4	2,300	45°	In the center of the chamber
	5	2,500		
	6	2,800		
3	7	2,300	90°	In the center of the chamber
	8	2,500		
	9	2,800		
4	10	2,300	90°	In the middle of 1 of the sides
	11	2,500		
	12	2,800		

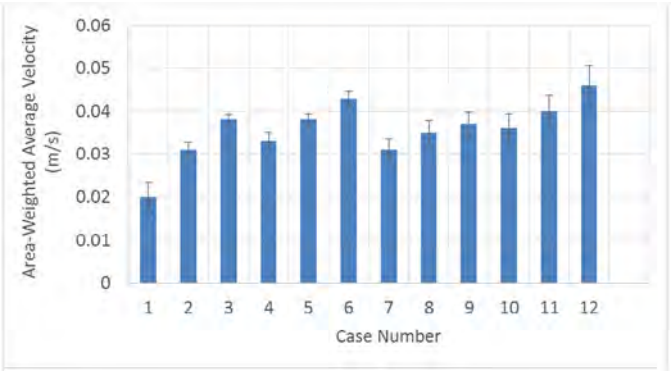

Fig 9. Average and standard variation of area-weighted average velocities on 5 different planes for 12 cases.

To have a better quantitative comparison between states, area-weighted average velocities were calculated on 5 different planes (Fig 9). The average and coefficient of variation (CV) of area-weighted velocities on 5 planes were calculated for each case and are reported in Table 2. Case 3 of state 1 had the smallest CV (6.5%), implying that the fan created the most uniform airflow when positioned in the middle of 1 side of the chamber at an angle of 45° and a speed of 2,800 rpm.

Bacteria were nebulized into the chamber through a port for 600 seconds at a rate of 5,000 CFU/min. For each of the 12 cases, the average of particle concentration in 5 volumes and its CV were calculated 600 seconds after completing the nebulization process (Table 3). Figure 10 shows the average particle concentration in the 5 volumes analyzed and the corresponding standard deviation. Case 3 had the lowest CV, implying that the bacterial distribution in this case was the most uniform. This is in line with our finding from analysis of the area-weighted average velocities. The small standard deviation and CV between the 5 volumes implies that, after 900 seconds, bacteria would be distributed uniformly inside the chamber,

Table 2
Area-weighted average velocity magnitude on 5 different planes for different cases

	State 1			State 2			State 3			State 4		
Case	1	2	3	4	5	6	7	8	9	10	11	12
Speed (rpm)	2,300	2,500	2,800	2,300	2,500	2,800	2,300	2,500	2,800	2,300	2,500	2,800
Plane 1	0.015	0.026	0.036	0.032	0.038	0.043	0.029	0.032	0.035	0.031	0.034	0.039
Plane 2	0.017	0.029	0.036	0.033	0.039	0.043	0.035	0.039	0.039	0.041	0.045	0.052
Plane 3	0.025	0.034	0.041	0.03	0.037	0.047	0.035	0.038	0.042	0.045	0.050	0.059
Plane 4	0.012	0.030	0.036	0.03	0.034	0.038	0.035	0.039	0.040	0.029	0.032	0.037
Plane 5	0.028	0.034	0.040	0.040	0.042	0.044	0.024	0.026	0.028	0.034	0.037	0.043
Mean	0.020	0.031	0.038	0.033	0.038	0.043	0.031	0.035	0.037	0.036	0.040	0.046
CV (%)	34.02	11.08	6.55	12.49	7.67	7.54	16.06	16.34	14.97	18.84	19.09	20.16

CV, coefficient of variation.

Table 3
Log_{10} colony forming units per meters^3 in 5 different volumes at 900 seconds for 12 cases

State	Case	Speed (rpm)	Volume 1	Volume 2	Volume 3	Volume 4	Volume 5	Average	CV (%)
1	1	2,300	4.685	4.565	4.636	4.562	4.679	4.626	0.64
	2	2,500	4.674	4.568	4.620	4.601	4.688	4.630	0.54
	3	2,800	4.662	4.597	4.630	4.631	4.700	4.644	0.42
2	4	2,300	4.678	4.592	4.661	4.541	4.685	4.631	0.67
	5	2,500	4.663	4.570	4.687	4.555	4.692	4.633	0.71
	6	2,800	4.639	4.566	4.725	4.590	4.709	4.646	0.76
3	7	2,300	4.722	4.551	4.664	4.522	4.676	4.627	0.93
	8	2,500	4.713	4.542	4.706	4.556	4.683	4.640	0.90
	9	2,800	4.692	4.497	4.718	4.575	4.697	4.636	1.03
4	10	2,300	4.747	4.564	4.668	4.544	4.692	4.643	0.93
	11	2,500	4.724	4.536	4.674	4.570	4.6988	4.640	0.89
	12	2,800	4.685	4.528	4.695	4.610	4.715	4.647	0.83

CV, coefficient of variation.

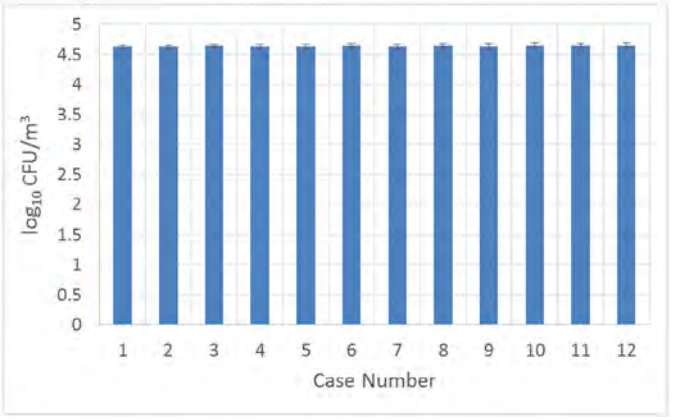

Fig 10. Average and standard variation of bacterial concentration in the 5 volumes analyzed after 900 seconds for 12 cases.

and there may not be any significant difference among the bacteria concentrations in the 5 different volumes analyzed.

The concentration of aerosolized bacteria in each volume was calculated over time for the optimum case (case 3). Table 4 summarizes the results. Figure 11 shows log_{10} colony forming units per meters^3 of samples over the 900 seconds of nebulization of the bacterial suspension into the chamber. The bacteria concentrations in the 5 volumes analyzed were different at the beginning of the process, but the curve of the 5 volumes converged after finishing the nebulization at 600 seconds and reached steady state at 900 seconds. This implies that 300 seconds (5 minutes) of stabilization time after completion of the nebulizing process will result in a uniform distribution of bacteria inside the chamber. That is, the bacteria are uniformly distributed, their concentration has reached a plateau, and the air sampling process can start.

Table 4
Bacteria concentration (CFU/m^3) in 5 volumes

Time (s)	Volume 1	Volume 2	Volume 3	Volume 4	Volume 5
100	1,925	6,865	6,055	2,160	3,195
200	4,315	11,795	10,310	4,965	7,275
300	12,270	21,850	17,405	10,160	16,380
400	21,575	26,960	19,855	17,725	26,120
500	29,475	31,570	33,435	28,430	35,605
600	36,710	40,685	39,695	35,110	41,815
700	48,330	42,740	41,115	38,585	49,575
800	41,860	40,105	43,320	41,010	48,660
900	45,955	39,530	42,655	42,745	50,115

Analysis of variance was performed to determine whether the bacteria concentrations in the 5 volumes analyzed over the time were significantly different. The results showed that the bacteria concentrations were the same at a 99% confidence level ($F_{4,40} = 0.29$; $P = .88$), implying that each of these 5 volumes could be used as a sampling site to calculate the airborne bacteria concentration inside the chamber.

To study the influence of the furniture on bacteria distribution in the chamber, the fan was positioned at the optimum location at a 45° angle at 2,800 rpm (state 1, case 3). Figure 12 shows the schematics of the room with the furniture.

As with the room without furniture, 600 seconds nebulizing time and 300 seconds stabilizing time were considered, and the bacteria concentrations in the 5 volumes were analyzed. The results are summarized in Table 5.

Figure 13 shows log_{10} colony forming units per meters^3 for 900 seconds after initiating bacterial nebulization into the chamber. The concentrations were different at the beginning of the nebulization process but converged during the stabilization time and reached a plateau at the end of the stabilization time.

The bacteria concentrations in the 5 volumes during the nebulization and stabilization processes in the chamber with furniture

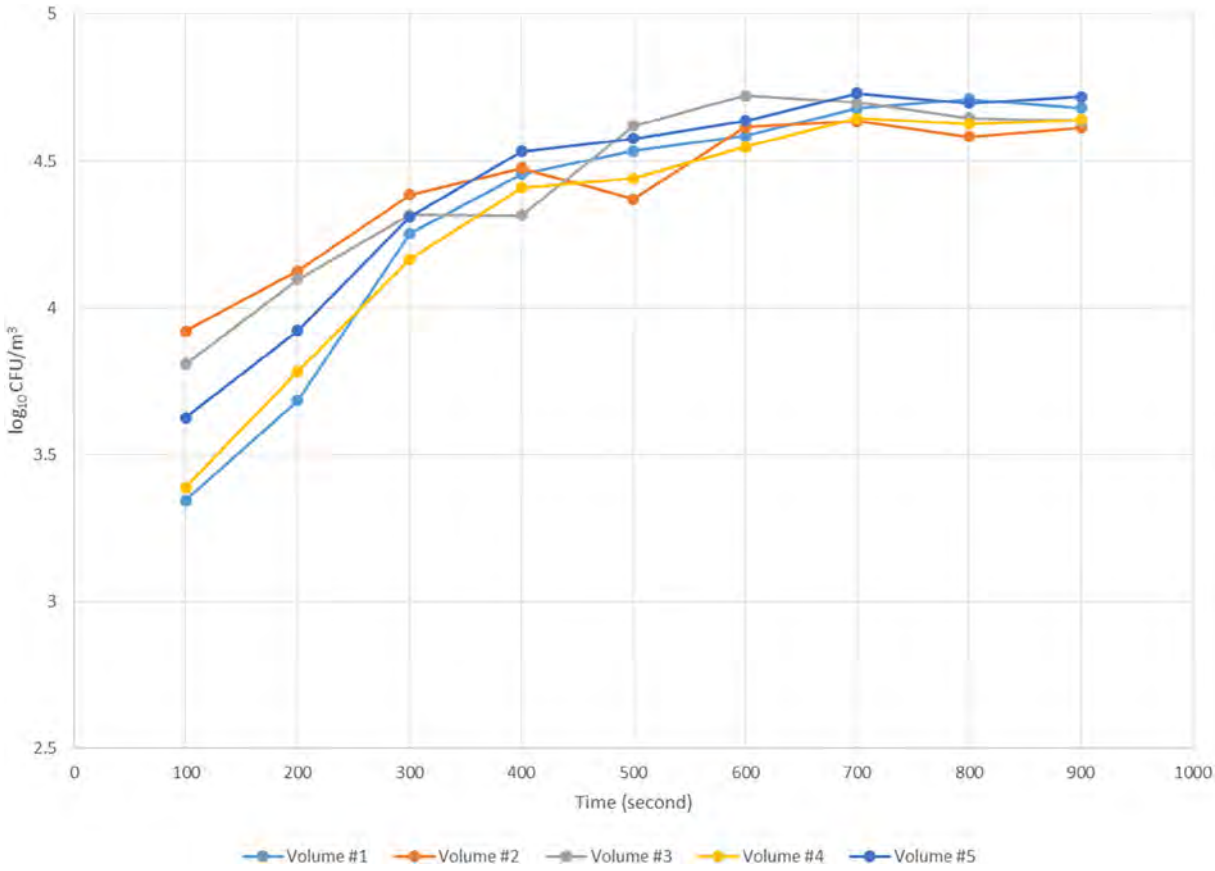

Fig 11. Log_{10} colony forming units per meters^3 in 5 volumes during nebulization and stabilization process. *CFU*, colony-forming units.

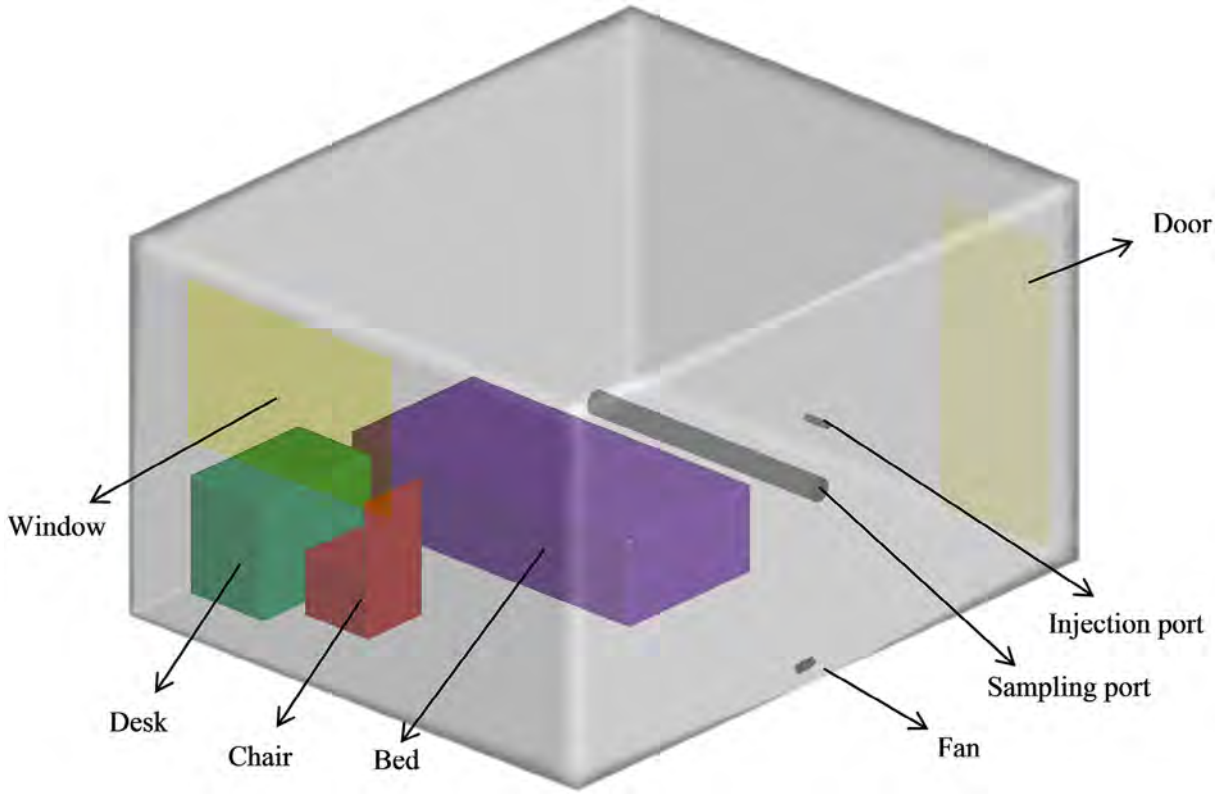

Fig 12. Aerobiology chamber with furniture.

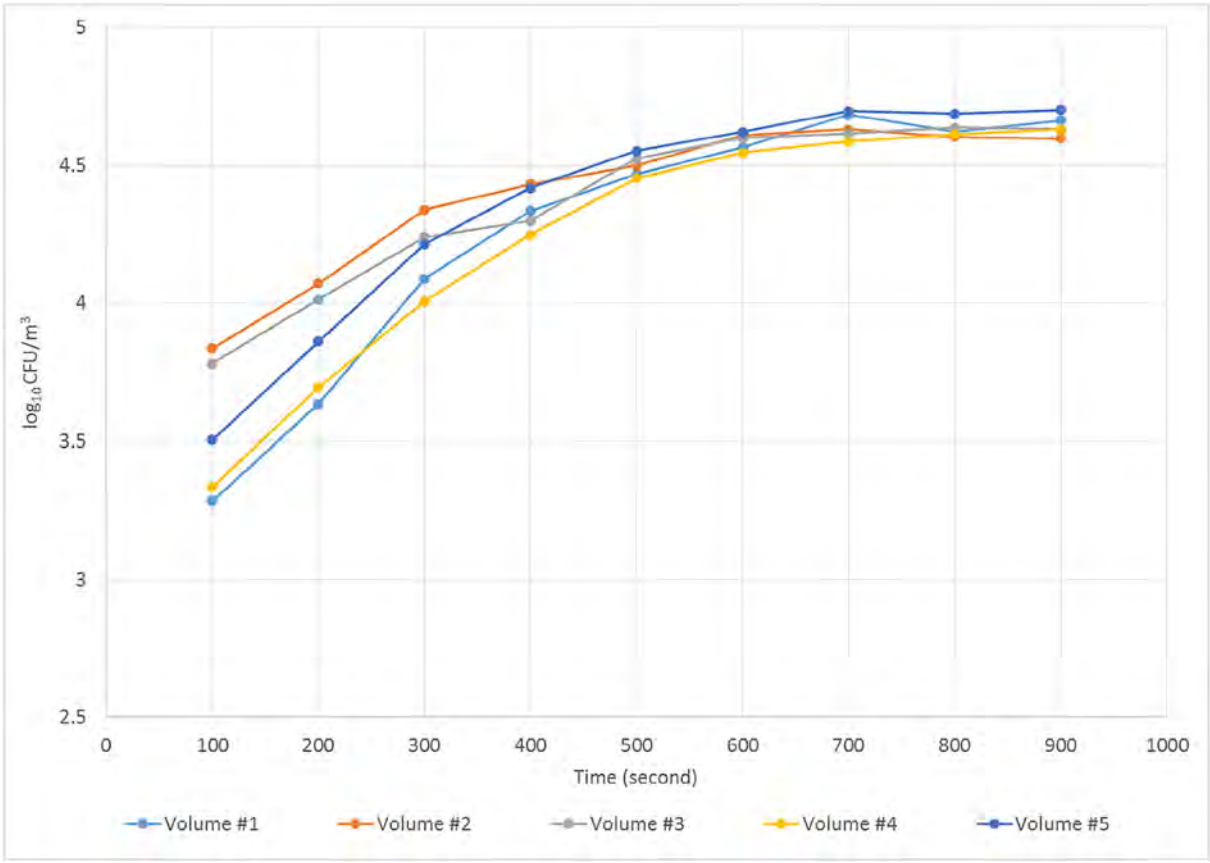

Fig 13. Bacterial concentration in the 5 different volumes analyzed during nebulization and stabilizing times in a chamber with furniture.

Table 5
Bacterial concentration (CFU/m^3) in the 5 different volumes analyzed with room furniture

Time (s)	Volume 1	Volume 2	Volume 3	Volume 4	Volume 5
100	2,215	8,340	6,455	2,445	4,235
200	4,850	13,355	12,530	6,070	8,390
300	17,945	24,250	20,705	14,650	20,445
400	28,550	29,960	20,645	25,685	34,080
500	34,210	23,470	41,645	27,590	37,745
600	38,480	41,280	52,695	35,280	43,415
700	47,730	43,240	49,915	44,230	53,715
800	51,460	38,300	44,310	42,280	49,810
900	47,980	41,005	43,210	43,695	52,430

were compared using analysis of variance. The bacteria concentrations in the 5 volumes were the same at the 99% confidence level ($F_{4,40} = 0.23$; $P = .99$). This implies that, in the presence of the furniture, a single sampling site is sufficient to represent the bacteria distribution inside the chamber.

CONCLUSIONS

Environmental Protection Agency guidelines simply recommend the use of a sealed and empty 800-ft^3 chamber for testing indoor air decontamination technologies, without further specifications on design or operation. However, we considered additional details, such as the time needed for producing a uniform distribution of test bacteria in the chamber with and without basic furniture and the position and number of sites for sampling air from within the chamber. This modeling study, based on CFD, was undertaken to address those issues. Our main conclusions are as follows:

- A muffin fan placed at a 45° angle at the bottom of 1 side of a chamber and operating at 2,800 rpm can provide sufficient air turbulence for uniform bacteria distribution throughout, even in the presence of basic room furniture.
- A 5-minute postnebulization time is sufficient to distribute introduced bacteria aerosols uniformly throughout a chamber.
- Simulating the collection of airborne bacteria from 5 different locations in the chamber indicated that a single site at the center of the chamber was sufficient to provide a representative profile of the concentration of the airborne bacteria.

This information should contribute to further standardization of the design and operation of aerobiology chambers for data generation on the airborne survival of human pathogens, as well as technologies for decontamination of indoor air.

References

1. Domgin JF, Huilier D, Burnage H, Gardin P. Coupling of a Lagrangian model with a CFD code: application to numerical modeling of the turbulent dispersion of droplets in a turbulent pipe flow. J Hydraul Res 1997;35:473-90.
2. Holmberg S, Li Y. Modeling of the indoor environment—particle dispersion and deposition. Indoor Air 1998;8:113-22.
3. Lai ACK. Particle deposition indoors: a review. Indoor Air 2004;12:211-24.
4. Zhang N. Motion and distribution of micro-sized solid particles in turbulent gas flow [PhD dissertation]. Manhattan, KS: Kansas State University; 2005.
5. Gao NP, Niu JL. Modeling particle dispersion and deposition in indoor environments. Atmos Environ 2007;41:3862-76.
6. Heederik D, Sigsgaard T, Thorne PS, Kline JN, Avery R, Bønløkke JH, et al. Health effects of airborne exposures from concentrated animal feeding operations. Environ Health Perspect 2007;115:298-302.
7. Just N, Duchaine C, Singh B. An aerobiological perspective of dust in cagehoused and floor-housed poultry operations. J Occup Med Toxicol 2009;4:13.
8. Memarzadeh F. Effect of reducing ventilation rate on indoor air quality and energy cost in laboratories. J Chem Health Saf 2009;16:20e6.

9. Ninomura P, Rousseau C, Bartley J. Updated Guidelines for Design and Construction of Hospital and Health Care Facilities. ASHRAE J 2006;48:H33-H37.
10. Zhang Y. Indoor air quality engineering. New York (NY): CRC Press; 2004.
11. American Society for Heating, Refrigeration & Air Conditioning Engineers. Position Document on Airborne Infectious Diseases. Atlanta (GA): ASHRAE; 2014.
12. Memarzadeh F, Xu W. Role of air changes per hour (ACH) in possible transmission of airborne infections. Build Simul 2012;5:15-28.
13. Qian H, Li Y, Nielsen PV, Hyldgaard CE, Wong TW, Chwang ATY. Dispersion of exhaled droplet nuclei in a two-bed hospital ward with three different ventilation systems. Indoor Air 2006;16:111-28.
14. Lin Z, Wang J, Yao T, Chow TT, Fong KF. Numerical comparison of dispersion of human exhaled droplets under different ventilation methods. World Rev Sci Technol Sustain Dev 2013;10:142-61.
15. Li Y, Leung GM, Tang JW, Yang X, Chao CY, Lin JZ, et al. Role of ventilation in airborne transmission of infectious agents in the built environment—a multidisciplinary systematic review. Indoor Air 2007;17:2-18.
16. Lai ACK, Cheng YC. Study of expiratory droplet dispersion and transport using a new Eulerian modeling approach. Atmos Environ 2007;41:7473-84.
17. Qian H, Li Y, Nielsen PV, Hyldgaard CE. Dispersion of exhalation pollutants in a two-bed hospital ward with a downward ventilation system. Build Environ 2008;43:344-54.
18. McNeil J, Zhai Z. Critical review on hospital surgical room and mechanical systems designs. World Rev Sci Technol Sustain Dev 2013;10:5-16.
19. Faulkner WB, Memarzadeh F, Riskowski G, Hamilton K, Chang CZ, Chang JR. Particulate concentrations within a reduced-scale room operated at various air exchange rates. Build Environ 2013;65:71-80.
20. Abduladheem A, Sahari KSM, Hasini H, Ahmed W, Mahdi RA. Ventilation air distribution in hospital operating room-review. Int J Sci Res (IJSR) 2013;2.
21. Zhai Z, Osborne AL. Simulation-based feasibility study of improved air conditioning systems for hospital operating room. Front Archit Res 2013;2:468-75.
22. Zhao B, Zhang Z, Li XT. Numerical study of the transport of droplets or particles generated by respiratory system indoors. Built Environ 2005;40:1032-9.
23. Liddament MW. *A Review of Building Air Flow Simulation*. Technical Note AIVC33. Air Infiltration and Ventilation Center. Coventry, Great Britain: University of Warwick Science Park; 1991.
24. Haghighat F, Jiang Z, Wang JCY, Allard F. Air movement in buildings using computational fluid dynamics. Trans ASME 1992;114:84-92.
25. US Environmental Protection Agency. Air sanitizers—efficacy data recommendations. Test guideline no. #OCSPP 810.2500-Air Sanitizers-2013-03-12 [EPA 730-C-11- 003]. Environmental Protection Agency website. 2012. Available from: http://www.noticeandcomment.com/-ocspp-810-2500-air-sanitizers-2013-03-12-epa-730-c-11-003-fn-24288.aspx. Published March 13, 2013. Accessed December 4, 2015.
26. Sattar SA, Kibbee RJ, Zargar B, Wright KE, Rubino JR, Ijaz MK. Decontamination of indoor air to reduce the risk of airborne infections: studies on survival and inactivation of airborne pathogens using an aerobiology chamber. Am J Infect Control 2016; [Epub ahead of print].
27. Ansys Fluent v.12.0 User manual, Available from: http://users.ugent.be/~mvbelleg/flug-12-0.pdf
28. Soltani M, Chen P. Shape design of internal flow with minimum pressure loss. Adv Sci Lett 2009;2:347-55.